Geometric Derivation of the Spectrum of Vacuum

Hans-Otto Carmesin[1,2,3]

[1](University Bremen, Germany)
[2](Studienseminar Stade, Germany)
[3](Observatory and Gymnasium Athenaeum Stade, Germany)

ABSTRACT: *In our universe, distances have increased since the Big Bang. This is directly indicated by the redshift of distant galaxies or of the cosmic microwave background. Usually, that increase of distances is explained by a continuous expansion of space according to general relativity. However, that explanation is very incomplete. This is indicated by the era of cosmic 'inflation'. In addition, the explanation of that era by the standard model of cosmology is hypothetic, problematic and not based on a fundamental concept. In contrast, the era of cosmic 'inflation' is derived and explained by physically founded phase transitions by a discontinuous change of space. These phase transitions provide the spectrum of the vacuum. With it, the density of vacuum is derived here. Moreover, the local value of the Hubble constant has been derived on the basis of that spectrum. Furthermore, many basic problems in elementary particle physics and in fundamental interactions have been solved by using that spectrum. For instance, the Higgs mechanism and the vacuum expectation value of elementary particle physics have been derived and explained. In this paper, we present a geometric derivation of the spectrum of vacuum. This provides further evidence and clarity.*

KEYWORDS – *cosmology, vacuum, spectrum, phase transitions, geometry, dark energy, quantum gravity*

I.   INTRODUCTION

The understanding of space is a basic and essential issue of research in mankind. That research ranges from Euclidean Geometry, via the discovery of continuous curvature of space and time in general relativity, GR, towards the expansion of space since the Big Bang in GR and in the standard model of cosmology, SMC [1-9]. Note that the basic concept of the Big Bang is founded by empirical evidence (see e. g. [1,2,8]) and by theory [5-12]. Thereby, the rate of expansion is characterized by iteratively improved concepts of the Hubble constant.

However, the description that is favored at present exhibits essential limitations [5-9]: GR explains the increase of distances since the Big Bang in a very incomplete manner, see section II (see e. g. [10], [11] p. 187 or [12] p. 41). Similarly, the SMC tries to explain that increase of distances since the Big Bang by a combination of GR and an era of a hypothetic cosmic 'inflation' [13,9,14]. However, that hypothetic cosmic 'inflation' is hardly founded, it causes the so-called 'reheating problem', and it requires the execution of fits of parameters that can hardly be explained in a fundamental manner [14].

In contrast, we derive the full increase of distances since the Big Bang, see the green triangles and line in figure (1) and see section III. Thereby, we do not execute any fit, we achieve precise accordance with observation, and we provide a founded explanation. In particular, we use one measured value, the time since the Big Bang. This value cannot be derived theoretically, as it is a peculiar value. The other used parameters have been derived theoretically in the framework of the present theory [12,15]. Thereby, the theoretically derived values are within the errors of measurement.

In order to explain the increase of distances since the Big Bang, we derive dimensional phase transitions. These transitions have been founded physically by gravity and relativity. In particular, four very general and very different and mutually independent models have been used [10,15,16,17]. Here, we provide a geometric derivation additionally, see section IV. Note that physics in higher dimension has been observed experimentally [18,19]. Moreover, we analyze essential geometric properties of these physically founded phase transitions, see sections V, VI and VII. These geometric properties include the dimensional distance enlargement factor and the observed rapid enlargement of distances in the early universe. This enlargement explains the era of the so-called cosmic 'inflation', whereby the hypothetic 'inflation' is replaced by the physically founded dimensional phase transitions.

Furthermore, we propose physically founded zero-point oscillations, ZPOs, that represent the vacuum [12,15,16,20,21]. Hereby, we derive geometric properties of these ZPOs, such as directions of propagation and

elongation, see section VIII. Thereby, we obtain the corresponding zero-point energies, ZPEs. These ZPEs represent the spectrum of the vacuum.

In 1998, the density of the vacuum has been discovered [22,23]. Meanwhile, that density has been confirmed by many very different methods of observation [8,24-34]. However, the physical nature of that density was a mystery [11,35]. Based on our spectrum of the vacuum, we derive the density of the vacuum, see section IX. Thereby, we execute no fit, and our theoretical density is within the errors of measurement, see figure (4). Note that this density has been derived alternatively by the dynamics of the vacuum, which has been represented by a differential equation, whereby that dynamics additionally represents the Schrödinger equation and quantum physics [12,16,36,37].

In 2022, it has been observed that the Hubble constant depends on space or time or on both, whereby a significance above five standard deviations has been achieved [38]. That dependence has been observed at smaller significance by many observers on the basis of very different methods of observation (see [24-34,39-45] and figure 4). Based on the spectrum derived here, the Hubble constant as a function of the redshift has been deduced, see section IX [16,45]. Thus, the observed local value of the Hubble constant has been explained on the basis of the present spectrum of vacuum. Thereby, no fit has been executed, and the derived theoretical density is within the errors of measurement, see figure (4).

Moreover, the spectrum of vacuum derived here has been used in order to deduce and explain many essential and fundamental concepts and quantities in elementary particle physics (see [12,36,37,46], section X).

II.   PROBLEM OF INCOMPLETENESS

The expansion of the universe since the Big Bang has been observed by various usual methods [1,2,8,23-34]. Moreover, that expansion has been modelled on the basis of general relativity, GR, [5-8]. However, these models and GR are not complete, see Fig. (1):
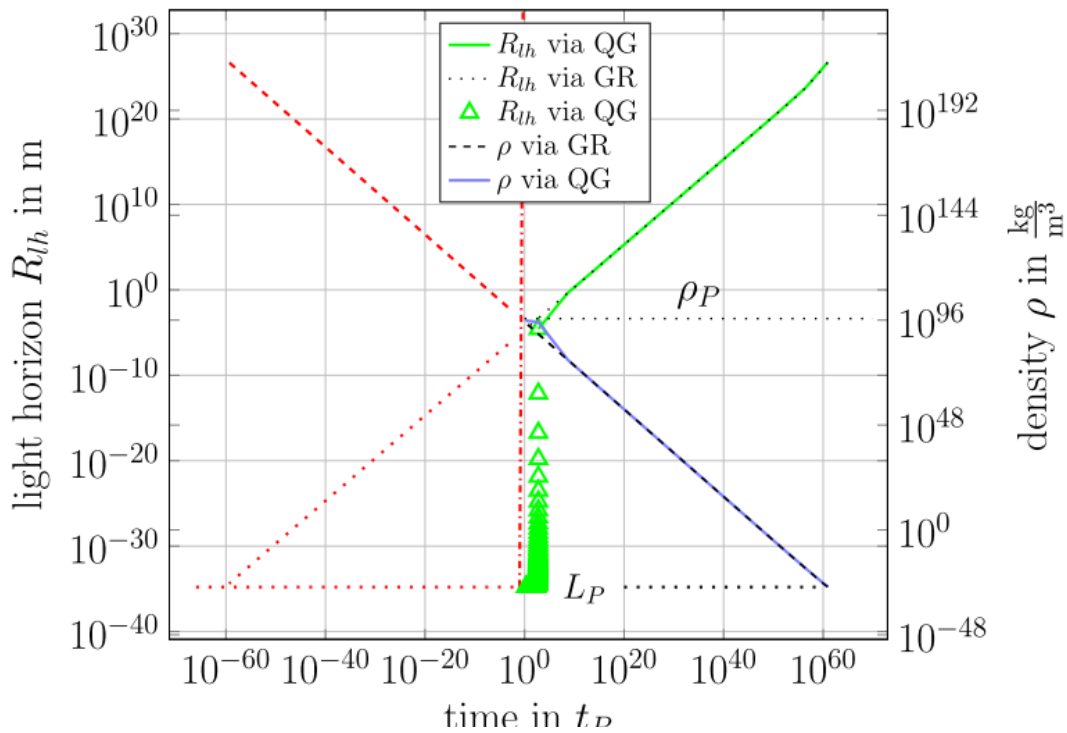
Fig. 1: Time evolution of the light horizon $R_{lh}(t)$ (green) and of the density $\rho(t)$ (blue) as a function of time in Planck times t_p: The density can only take values below the Planck density ρ_P. Thus, the time evolution can be traced back from $t/t_p \approx 10^{60}$ towards $t/t_p \approx 1$ only. Hence, times towards $t/t_p \approx< 1$ are not physically meaningful (red). However, at $t/t_p \approx 1$ and according to general relativity, GR, the value of the light horizon is $R_{lh} \approx 10^{-4}$ m. Thus, <u>GR is very incomplete</u>, as a complete time evolution must range from is $R_{lh} \approx 10^{26}$ m towards is $R_{lh} = L_P = 1.616 \cdot 10^{-35}$ m. Quantum gravity, QG, solves that incompleteness, see triangles ([12], Fig. 2.4): At the Big Bang, the light horizon starts at approximately the Planck length, $R_{lh} \approx L_P$. Then the light horizon increases slightly by the formation of vacuum, and it increases in a very rapid manner at a series of dimensional phase transitions (triangles, according to QG). These transitions do not cause an increase of the volume. Later, the light horizon increases in three-dimensional space by the formation of vacuum and volume (green line). Altogether, GR is very incomplete, whereas <u>QG solves that incompleteness</u>.

Complete physics is characterized at least by the combination of gravity and quantum physics [10-12,15,16,36,37]. In that framework of quantum gravity, physical systems range from the Planck length $L_P = 1.616 \cdot 10^{-35}$ m to the present-day light horizon at $R_{lh} = 4.1 \cdot 10^{26}$ m. Moreover, the Planck density $\rho_P = 5.155 \cdot 10^{96}$ kg/m^3 cannot be exceeded in nature [12,15,16]. So, in a complete physical system, the Planck length can be achieved. However, according to general relativity, the present-day light horizon would never have been smaller than 0.005 mm, as at that radius, the density of the universe would be equal to the Planck density. So, a further reduction of R_{lh} would be impossible, see figure (1) and [12,15,16].

III. SOLUTION BY DIMENSIONAL PHASE TRANSITIONS

In this section, we summarize the solution of the above problem of incompleteness by dimensional phase transitions. According to an advanced analysis within quantum gravity, the above incompleteness of GR is solved, thereby the light horizon has reached the Planck length, $R_{lh} \approx L_P$. This is achieved by a series of dimensional phase transitions (see e.g. [12,15,16]).

So far, these phase transitions have been derived by five methods: a van der Waals type analysis of two objects (see e.g. [12,15,16]), a transition in a Bose gas (see e.g. [16]), a phase transition of connections (see e.g. [16]), a theory of the dark energy (see e.g. [12,15,16,20,21]) and a droplet model (see e.g. [17]). In all models, a dimensional phase transition does not cause a change of the volume.

IV. INVARIANCE OF THE VOLUME AT A DIMENSIONAL PHASE TRANSITIONS

In the above section, we realized that a dimensional phase transition does not cause a change of the volume. Thereby, we used results provided by four models of dimensional phase transitions. In this section, we derive that fact even without a model of the phase transition.

The time evolution of the light horizon $R_{lh}(t)$ implies that a dimensional phase transition does not cause a change of the volume:

The time evolution of the light horizon $R_{lh}(t)$ is analysed from the present-day time t_0 backwards in time.

Thereby, the light horizon $R_{lh}(t)$ decreases. Thus, the volume $\frac{4\pi}{3}R_{lh}^3(t)$ within the light horizon decreases. Hereby, the energy (including mass $m = E/c^2$) is a conserved quantity, whereby this holds even in the presence of the redshift and the formation of vacuum [11,47]. Hence, the density $\rho(t)$ increases. This process takes place according to GR.

As a consequence, according to that process, there occurs a smallest possible value of the light horizon. We name that value R_1. That value R_1 is reached, when the density $\rho(t)$ reaches the maximal possible density ρ_{max}:

$$When\ \rho(t) = \rho_{max},\ then\ R_{lh}(t) = R_1 \qquad (1)$$

Note that the maximal possible density ρ_{max} is equal to one half of the Planck density ρ_P (see e.g. [12,15,16]):

$$\rho_{max} = \rho_P/2 \qquad (2)$$

The precise value R_1 depends on the details of the used cosmological model. Hereby, the usual cosmological models derived from GR exhibit a value R_1 that is in the vicinity of one tenth of a millimetre (see e.g. [12,15,16] and figure (1)):

$$R_1 \approx 0.1\ mm \qquad (3)$$

In a complete time evolution of the light horizon $R_{lh}(t)$, the value of $R_{lh}(t)$ reaches the smallest value that can be observed by a single measurement, the Planck length L_P, when the analysis is performed backwards in time:

The time evolution of the light horizon $R_{lh}(t)$, analysed backwards from R_1 towards the Planck length L_P can be achieved by physically founded dimensional phase transitions (see e. g. [15,16,17]). Hereby, the density has already the maximal possible value, see equation (1). Thus, a dimensional phase transition cannot cause an increase of the density. Hence, a dimensional phase transition cannot cause a decrease of the volume. Moreover, the time evolution of the light horizon $R_{lh}(t)$ does not increase the volume, when that time evolution is analysed backwards in time. Thence, a dimensional phase transition can neither decrease nor increase the volume. So, a dimensional phase transition does not cause any change of the volume. For details about the dimensional phase transitions, see e. g. [10-12,15-17]. For observations of higher dimensions, see e. g. [18,19].

In the next sections, we derive the geometric properties of the physically founded dimensional phase transitions.

V. BASIC GEOMETRIC RELATIONS AT DIMENSIONAL PHASE TRANSITIONS

In this section, we introduce the basic geometric relations that characterize a dimensional phase transition.

Firstly, there is a smallest length L_P that can be observed or measured at a single measurement. Physically, that length is the Planck length L_P. A quantity, that is scaled according to the Planck length, is marked by a tilde. For instance, a scaled length $\tilde{L}$ is marked as follows:

$$\tilde{L} = \frac{L}{L_P} \tag{4}$$

Thereby, the smallest measurable line segment has a scaled length two, as a measurable line segment must have distinct start and end points:

$$\tilde{L} \geq 2 \tag{5}$$

Secondly, as a consequence, at a dimension D, a hypercube with a length $\tilde{L}_D$ has the following scaled volume:

$$\tilde{V}_D = \tilde{L}_D^D \tag{6}$$

Note that we use a hypercube as an appropriate tool for the analysis of ratios of lengths and volumes.

Thirdly, at a dimensional phase transition, a hypercube changes its dimension, whereby the volume of the hypercube remains invariant. For instance, at a dimensional phase transition from a dimension $D + s$ to a dimension D, the following relation holds:

$$\tilde{V}_D = \tilde{V}_{D+s} \tag{7}$$

Fourthly, as a consequence, the length $\tilde{L}_D$ of a hypercube at a dimension D decreases, if that hypercube experiences a dimensional phase transition to a higher dimension $D + s$:

$$\tilde{L}_D \geq \tilde{L}_{D+s} \tag{8}$$

VI. DISTANCE ENLARGEMENT FACTOR

At a dimensional phase transition from a dimension $D + s$ to a dimension D, the length $\tilde{L}_{D+s}$ of a hypercube increases by a factor $Z_{D+s \to D}$. That factor is named dimensional distance enlargement factor. In this section, we analyze the factor:

$$Z_{D+s \to D} = \frac{\tilde{L}_D}{\tilde{L}_{D+s}} \tag{9}$$

At a dimensional phase transition from a dimension $D + s$ to a dimension D, and as a consequence of equations (6) and (7), the edges of a hypercube obey the following relation:

$$\tilde{L}_D^D = \tilde{L}_{D+s}^{D+s} \tag{10}$$

We apply equation (10) to the dimensional distance enlargement factor in equation (9):

$$Z_{D+s \to D} = \tilde{L}_{D+s}^{s/D} \tag{11}$$

In general, at a dimensional phase transition from a dimension $D + s$ to a dimension D, the length $\tilde{L}_{D+s}$ of a line segment is not invariant, as the volume of a hypercube is invariant, see equations (7) and (8). Correspondingly, the length $\tilde{L}_{D+s}$ of a line segment is transformed according to the dimensional distance enlargement factor in equation (11).

As a consequence, if a line segment has the length 2 in a dimension D, then that line segment cannot take part in a dimensional phase transition to a higher dimension $D + s$, as the length would decrease at such a transition, see equation (8).

In particular, if the shortest diameter $2 \cdot \tilde{R}_1$ corresponding to the shortest light horizon $\tilde{R}_{D=3,lh}$ at dimension three, see figure (1), evolves towards the value two at a higher dimension D, then that diameter $2 \cdot \tilde{R}_{D,lh} = 2$ cannot experience a dimensional phase transition to a higher dimension $D + s$. That dimension D is named the dimensional horizon D_{hori}.

$$2 \cdot \tilde{R}_{D_{hori},lh} = 2 \tag{12}$$

In order to derive the dimensional distance enlargement factor $Z_{D_{hori} \to 3}$, by which the diameter $2 \cdot \tilde{R}_{D_{hori},lh}$ is multiplied in order to become the value $2 \cdot \tilde{R}_1$, we use equation (11). Thereby, we apply the dimension $D + s = D_{hori}$, the dimension $D = 3$, the difference $s = D_{hori} - 3$, whereby the diameter two at the dimension D_{hori} is the scaled length in equation (11):

$$Z_{D_{hori} \to 3} = 2^{(D_{hori}-3)/3} \tag{13}$$

VII. CALCULATION OF THE DIMENSIONAL HORIZON

In this section, we calculate the value of the dimensional horizon. For it, we use the present-day value of the light horizon (see e. g. [8,15,16]):

$$R_{lh}(t_0) = 4.1 \cdot 10^{26} \text{ m} \tag{14}$$

Thus, the complete enlargement factor $q_{t_{horizon} \to t_0}$ ranging from the present-day time t_0 towards the time of the dimensional horizon $t_{horizon}$ is the following ratio:

$$q_{t_{horizon} \to t_0} = \frac{R_{lh}(t_0)}{L_P} = \frac{4.14 \cdot 10^{26}}{1.616 \cdot 10^{-35}} = 2.56 \cdot 10^{61} \tag{15}$$

The expansion of space is a uniform scaling with a scale factor $k_{t_{horizon} \to t_0}$ ranging from the present-day time t_0 towards the time of the dimensional horizon $t_{horizon}$. That factor can be derived from the corresponding densities of radiation $\tilde{\rho}_{r,t_{horizon}}$ and $\tilde{\rho}_{r,t_0}$ (see e. g. [12,15,16,20,21]):

$$\tilde{\rho}_{r,t_{horizon}} = 6.52 \cdot 10^{-127} \quad and \quad \tilde{\rho}_{r,t_0} = 0.5 \tag{16}$$

In particular, the scale factor is the fourth root of the ratio of these densities, according to the redshift (see e. g. [15,16]):
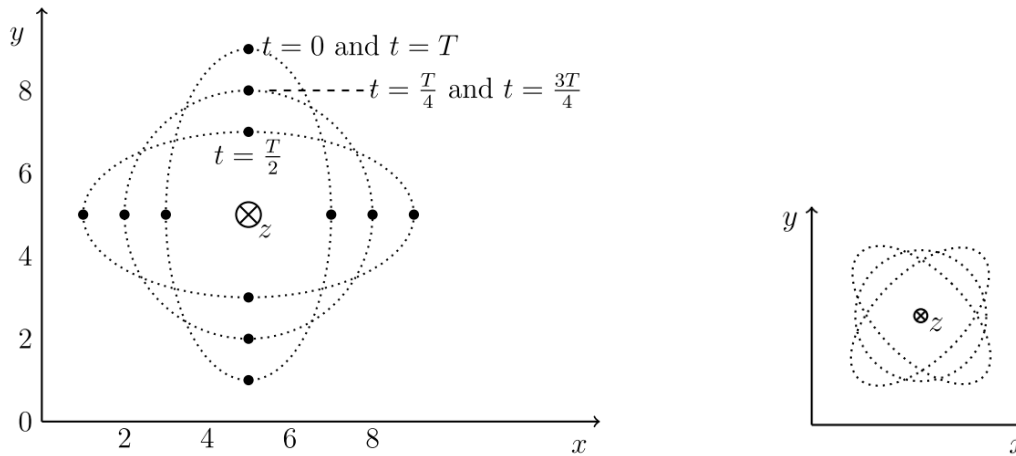
$$k_{t_{horizon} \to t_0} = \left(\frac{\tilde{\rho}_{r,t_{horizon}}}{\tilde{\rho}_{r,t_0}} \right)^{1/4} = 2.96 \cdot 10^{31} \tag{17}$$

Accordingly, the dimensional distance enlargement factor $Z_{D_{hori} \to 3}$ is the ratio:

$$Z_{D_{hori} \to 3} = \frac{q_{t_{horizon} \to t_0}}{k_{t_{horizon} \to t_0}} = 8.66 \cdot 10^{29} \tag{18}$$

The dimensional horizon is obtained by solving equation (13):

$$D_{hori} = \ln\left(Z_{D_{hori} \to 3} \right) \cdot \frac{3}{\ln 2} + 3 = 301.3 \approx 301 \tag{19}$$

Fig. 2: Gravitational wave: In three-dimensional space, a gravitational wave has a direction of propagation $\vec{k}$ and two transverse directions of elongation. These three directions are mutually orthogonal.

VIII.   SPECTRUM OF THE VACUUM

In this section, we derive the spectrum of the vacuum. For it, we use the plausible concept that a quantum of vacuum is a zero-point oscillation, ZPO, of a gravitational wave (see [12,15,16,20,21]).

Firstly, we develop a geometric description of a gravitational wave: In three-dimensional space, a gravitational wave has a direction $\vec{k}$ of propagation and two transverse directions of elongation (see figure 2). Thereby, these two transverse directions are orthogonal to each other, and they have a phase shift of π. For instance, in the left part of figure (2), the direction $\vec{k}$ of propagation is parallel to the z-axis, and the two transverse directions are parallel to the x-axis and to the y-axis. In another example (see right part of figure 2), the direction $\vec{k}$ of propagation is parallel to the z-axis, and the two transverse directions are parallel to the following vectors:

$$\vec{e}_1 = \begin{pmatrix} 1 \\ 1 \\ 0 \end{pmatrix} \quad and \quad \vec{e}_2 = \begin{pmatrix} 1 \\ -1 \\ 0 \end{pmatrix} \tag{20}$$

The second example can be reduced to the first example by rotating the coordinate system by an angle of $\pi/4 = 45°$. Accordingly, we analyze gravitational waves in an orthogonal coordinate system, in which the direction $\vec{k}$ of propagation is parallel to the last coordinate axis, while the transverse directions of elongation are parallel to the other coordinate axes. For instance, in a D dimensional space, the gravitational wave has one direction $\vec{k}$ of propagation and $D - 1$ transverse directions of elongation. Thereby, the direction $\vec{k}$ of propagation and all $D - 1$ transverse directions of elongation are mutually orthogonal. This physically founded

result provides a geometric description of a gravitational wave in a D dimensional space. In particular, the dimension D of space must be three or larger.

Secondly, we derive the gravitational wave at the dimensional horizon D_{hori}: At the dimensional horizon D_{hori}, the universe is at the Planck scale. Thus, the corresponding energy is one half of the Planck energy (see e. g. [12,15,16]):

$$E(D_{hori}) = \frac{E_P}{2} \quad or \quad \tilde{E}(D_{hori}) = \frac{1}{2} \tag{21}$$

That energy can be described in terms of the Planck circular frequency ω_P:

$$E(D_{hori}) = \frac{E_P}{2} = \hbar \cdot \omega_P \cdot \frac{1}{2} \tag{22}$$

Thus, the energy at the Planck scale is the zero-point energy, ZPE [11,12,15,16]. Correspondingly, the gravitational wave is a ZPO at the dimensional horizon D_{hori}.

Thirdly, we derive the time evolution of that ZPO or quantum of vacuum and of the corresponding ZPE: When the space expands according to GR, then the number of these quanta or ZPOs increases, whereby the ZPE remains invariant. However, at a dimensional phase transition from a dimension $D + s$ to a dimension D, the ZPE changes as follows: At a dimensional phase transition from a dimension $D + s$ to a dimension D, the number of transverse elongations changes from $D + s - 1$ to $D - 1$. Thus, s transverse directions of elongation are lost. That loss of elongations causes a loss of the energy by the factor $\frac{D-1}{D+s-1}$. Moreover, the quanta of vacuum represent the space. Correspondingly, each quantum of vacuum changes its wavelength according to the dimensional distance enlargement factor $Z_{D+s \to D}$. Thus, the ZPO increases by the factor $Z_{D+s \to D}$. Hence, the ZPO experiences the corresponding redshift, and the ZPE is divided by the factor $Z_{D+s \to D}$. Altogether, the ZPE of the vacuum, $ZPE_\Lambda(D)$, is changed by both factors as follows:

$$ZPE_\Lambda(D) = ZPE_\Lambda(D + s) \cdot \frac{D-1}{D+s-1} \cdot \frac{1}{Z_{D+s \to D}} \tag{23}$$
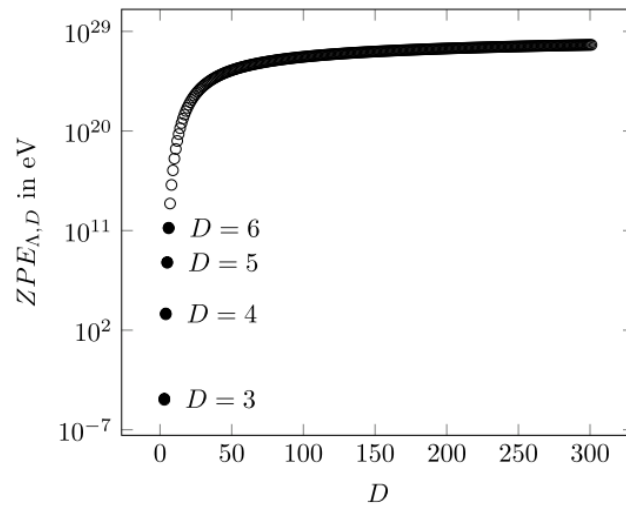
Fig. 3: Excitation spectrum: The zero-point energy, ZPE, of the quanta of vacuum is shown as a function of the dimension that occurred in the course of dimensional phase transitions in the early universe. As these phase transitions are founded on laws of physics and geometry, these ZPE represent the spectrum of vacuum in a general manner. For instance, that spectrum is essential, when elementary particles form in present-day reactions or when elementary interactions take place, such as the electromagnetic interaction in present-day electric equipment, see section X.

In particular, the $ZPE_\Lambda(D)$ can be determined by using the $ZPE_\Lambda(D_{hori})$ at the dimensional horizon. Hereby, we scale with the Planck energy:

$$\widetilde{ZPE}_\Lambda(D) = \widetilde{ZPE}_\Lambda(D_{hori}) \cdot \frac{D-1}{D_{hori}-1} \cdot \frac{1}{Z_{D_{hori} \to D}} \tag{24}$$

We use $\widetilde{ZPE}_\Lambda(D_{hori}) = \frac{1}{2}$:

$$\widetilde{ZPE}_\Lambda(D) = \frac{1}{2} \cdot \frac{D-1}{D_{hori}-1} \cdot \frac{1}{Z_{D_{hori} \to D}} \tag{25}$$

We apply the dimensional distance enlargement factor $Z_{D+s \to D}$ in equations (11, 12, 13):

$$\widetilde{ZPE}_\Lambda(D) = \frac{1}{2} \cdot \frac{D-1}{D_{hori}-1} \cdot 2^{-(D_{hori}-D)/D} = \frac{D-1}{D_{hori}-1} \cdot 2^{-D_{hori}/D} \tag{26}$$

In particular, for the case $D_{hori}=301$, we obtain the following spectrum of the vacuum:

$$\widehat{ZPE}_\Lambda(D) = \frac{D-1}{300} \cdot 2^{-301/D} \tag{27}$$

The corresponding spectrum in eV is obtained by multiplication by the Planck energy $E_P = 1,221 \cdot 10^{28}$ eV:

$$ZPE_\Lambda(D) = \widehat{ZPE}_\Lambda(D) \cdot E_P = \frac{D-1}{300} \cdot 2^{-\frac{301}{D}} \cdot E_P = (D-1) \cdot 2^{-301/D} \cdot 4,07 \cdot 10^{25} \text{ eV} \tag{28}$$

The above term for the energy $ZPE_\Lambda(D)$ of the quanta of vacuum holds according to the laws of physics and geometry. Thus, the present-day vacuum can be excited to any of these $ZPE_\Lambda(D)$. Hence, these $ZPE_\Lambda(D)$ represent possible excitation states of the present-day vacuum. That spectrum of excitation states of the vacuum is presented in figure (3).

IX.   GEOMETRIC DERIVATION OF THE DENSITY OF VACUUM

In order to obtain a test of the spectrum of the vacuum, we use the spectrum of vacuum, in order to derive the density ρ_Λ of the present-day vacuum, in this section. Remind the following essential facts about that spectrum:

Firstly, the spectrum of vacuum represents the complete time evolution of space, ranging from the dimensional horizon towards the present-day three-dimensional space at the present-day time t_0.

Secondly, the spectrum of vacuum is based on the underlying laws of physics and geometry. Thus, the spectrum can be applied to any physical system, in the past, at the present-day time, or in the future. Thereby, the spectrum of vacuum is also based on the light horizon, whereby that horizon is a causal horizon (no event outside that horizon can cause any influence upon our present-day life or physics). Note that this horizon presents a finite range of causality, whereby translation invariance still provides a potentially infinite space.

Thirdly, the properties of space are not assumed here. In contrast, the properties of space are derived here.

Firstly, we derive the volume $V(D)$ corresponding to a quantum of vacuum with its energy $ZPE_\Lambda(D)$. At the dimensional horizon D_{hori}, the universe is at the Planck scale. Thus, the corresponding energy is one half of the Planck energy. Moreover, an object has the smallest possible extension. So, the extension of an object is the length $2L_P$ of the smallest line segment, in each direction. Thus, that length $2L_P$ represents diameters, and the smallest object is a hyperball with radius L_P. Hence the corresponding volume is the volume of a hyperball with length $L = L_P$ (for details see e.g. [15,16]). For it, we name the volume of a hyperball with radius one by V_D. At a dimension D, the length of the cube has increased by the dimensional distance enlargement factor $Z_{D_{hori} \to D}$.

$$V(D) = V_D \cdot L_P^D \cdot Z_{D_{hori} \to D}^D \tag{29}$$

Secondly, we derive the density: The density ρ_Λ is equal to the scaled energy $\widehat{ZPE}_\Lambda(D)$ in equation (25) multiplied by the Planck energy, divided by the above volume and by the square of the velocity of light:

$$\rho_\Lambda(D) = \widehat{ZPE}_\Lambda(D) \cdot \frac{E_P}{V(D) \cdot c^2} = \frac{1}{2} \cdot \frac{D-1}{D_{hori}-1} \cdot \frac{1}{Z_{D_{hori} \to D}^{D+1}} \cdot \frac{E_P}{L_P^D \cdot c^2} \tag{30}$$

According to equations (29) and (13), for the present-day dimension $D = 3$, and for $D_{hori} = 301$, with $V_3 = 4\pi/3$, the above equation represents the following theoretical value for the density of the vacuum:

$$\rho_\Lambda(D = 3) = \frac{1}{300} \cdot \frac{1}{2^{(D_{hori}-3) \cdot 4/3}} \cdot \frac{E_P}{L_P^3 \cdot c^2 \frac{4\pi}{3}} = 7,6 \cdot 10^{-27} \frac{kg}{m^3} = \rho_{\Lambda,\text{theo}} \tag{31}$$

Thirdly, we prepare a comparison with observed values. According to the Friedmann-Lemaitre equation, and corresponding to the fact that the curvature parameter in that equation is equal to zero, the Hubble constant is the following function of the density:

$$H_{0,\text{obs}}^2 = \frac{8\pi G}{3} \cdot \left(\langle \rho_m \rangle + \rho_{\Lambda,\text{obs}} \right)$$

Hereby, the density has been expressed by the sum of the density of vacuum $\rho_{\Lambda,\text{obs}}$ and of the density of matter $\langle \rho_\text{m} \rangle$, averaged over the universe. Thereby, the density of radiation has been neglected, as it is negligibly small in the range of the usually observed values at redshifts above the redshift of the cosmic microwave background, CMB, $z_{CMB} = 1090$ [8].

Fourthly, equations (15) until (19) show that the dimensional horizon D_{hori} is a function of the time t after the Big Bang, in general. Thus, the dimensional horizon D_{hori} is a function of the redshift. As a consequence, see equation (30), the density of vacuum ρ_Λ is a function of the redshift. So, the above equation takes the following form:

$$H_{0,\text{obs}}^2(z) = \frac{8\pi G}{3} \cdot \left(\langle \rho_m \rangle + \rho_{\Lambda,\text{obs}}(z) \right) \tag{32}$$

Fifthly, it is essential to realize a very interesting finding: If an observer uses radiation that has been emitted at a redshift z, in order to measure the Hubble constant $H_{0,obs}(z)$, then the resulting observed value is a function of the redshift z. Note that this finding has been obtained at a significance of more than five standard deviations [38].

According to the Friedmann-Lemaitre equation, and corresponding to the fact that the curvature parameter in that equation is equal to zero, the Hubble constant is the following function of the density:

$$H_{0,obs}^2(z) = \frac{8\pi G}{3} \cdot \left(\langle \rho_m \rangle + \rho_{\Lambda,obs}(z) \right) \tag{32}$$

The observed values of the density of vacuum $\rho_{\Lambda,obs}(z)$ are obtained from the observed values $H_{0,obs}(z)$, by solving the above equation:

$$\rho_{\Lambda,obs}(z) = H_{0,obs}^2(z) \cdot \frac{3}{8\pi G} - \langle \rho_m \rangle \tag{33}$$

Sixthly, the corresponding theoretical values $\rho_{\Lambda,theo}(z)$ have been derived by an analysis of the time evolution of the dimensional horizon [12,15,16,20,21]: The time evolution of the dimensional horizon provides a time evolution of the spectrum in equation (24). Thus, the spectrum of the generated vacuum varies slightly as a function of time. Thus, the present-day vacuum is a mixture of quanta of vacuum at slightly different energies $ZPE_\Lambda(t)$. So, the present-day vacuum is a polychromatic vacuum.

Seventhly, we compare theoretical and observed values: In figure (4), the observed densities $\rho_{\Lambda,obs}(z)$ are presented by marks, the corresponding theoretical densities $\rho_{\Lambda,theo}(z)$ are presented by the dashed line, and the value derived here on the basis of the actual dimensional horizon $D_{hori} = 3$ is presented by the dot-dashed line. Furthermore, for the case of small redshifts $z < 0.04$, the probes used in the measurement have been emitted within our local attractor Laniakea. That attractor has an underdensity. So, the density of matter $\rho_{m,Laniakea}$ is below the averaged density of the universe $\langle \rho_m \rangle$. Hence, the density $\rho_{\Lambda,obs}(z)$ is additionally increased by the difference $\langle \rho_m \rangle - \rho_{m,Laniakea}$. That increase is marked by four arrows in figure (4).

Altogether, the geometric derivation of the density of vacuum applied here provides a value that is clearly within the range of measured values, see dot-dashed line in figure (4). Moreover, the geometric derivation of the spectrum has been used, in order to derive the theoretical values densities $\rho_{\Lambda,theo}(z)$. These are within the errors of measurement of the observed values presented in figure (4). This finding provides additional evidence for the spectrum derived here.
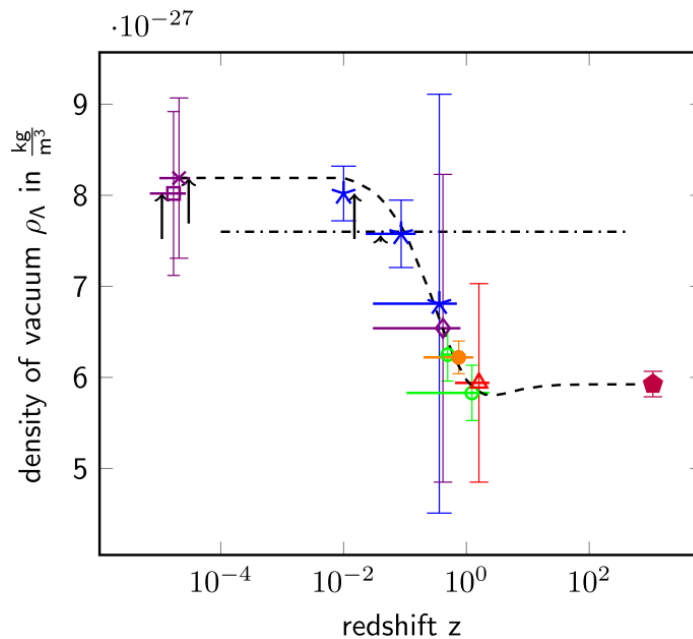
Fig. 4: Density of the vacuum ρ_Λ: Probes: X megamaser [24], □surface brightness [31], star: distance ladder [25,32,33,38], ◇ gravitational wave [30], o baryonic acoustic oscillations [26,27], ● weak gravitational lensing [28], Δ strong gravitational lensing [29], pentagon: CMB [8]. Local under-density of our local attractor Laniakea: arrows [39-45]. Theory: $- \cdot - \cdot - \cdot -$: based on actual dimensional horizon $D_{hori}(z=0) = 301$ $- - - - -$: time evolution of the dimensional horizon $D_{hori}(z)$ provides polychromatic vacuum. Summary: The theoretical values of the density of vacuum are within the errors of measurement.

X.   OUTLOOK

In this section, we summarize further essential results that have been derived from the present spectrum of vacuum.

(1) There occur additional excitation states: The transverse ZPOs derived above can be excited to longitudinal ZPOs. Moreover, each of these ZPOs can be excited by harmonic oscillations [12,16].

(2) Three longitudinal states in item (1) can bind to a triple, in order to form a three-dimensional object in three-dimensional space [12].

(3) The triples in item (2) include the Higgs boson. Hereby, the mass m_H of the Higgs boson is derived. Thereby, no fit is executed and the theoretical value is within the errors of measurement [12].

(4) The Higgs bosons in item (3) can bind to a pair. Such pairs have been observed at a significance of four standard deviations. The energy E_{pair} of that pair has been derived on the basis of the mass m_H of the Higgs boson in item (3). That energy is equal to the energy E_{vev} of the empirically found vacuum expectation value, vev. Thus, the vev has been derived and explained on the basis of the spectra derived here. Based on the vev, the Higgs mechanism has been derived and explained on the basis of the spectra derived here [37].

(5) The sum of the masses of the neutrinos has been derived and explained on the basis of the spectra derived here [12].

(6) It has been observed that neutrinos violate the symmetry of parity transformations. That fact means that neutrinos distinguish between left-handed and right-handed situations. The breaking of that symmetry has been derived and explained on the basis of the spectra derived here [37].

(7) The elementary particles in items (3) to (6) generate elementary and fundamental interactions such as the electromagnetic interaction or the weak interaction. These have been derived and explained on the basis of the spectra derived here [37,46].

(8) The density of vacuum has been derived by geometric methods here. Alternatively, that density has been derived on the basis of the dynamics. Thereby, the dynamics has been represented in the form of a differential equation. Hereby, also the theoretical values $\rho_{\Lambda,\text{theo}}(z)$ have been derived and explained [16,12,45].

XI.   DISCUSSION

The space has expanded since the Big Bang [1,2,8,34]. That expansion has usually been described and explained by general relativity, GR, and by the standard model of cosmology, SMC, [5-8]. However, in the early universe, distances increased in a very rapid manner, see figure (1). The era of that rapid increase has been named era of cosmic 'inflation' [13]. However, the concept of that 'inflation' is hypothetic and problematic, as it causes the 'reheating problem' and requires several parameters that are hardly founded in a fundamental physical manner [8,9,14]. So, the SMC describes that era in a hypothetic, problematic and hardly fundamental manner. Moreover, GR does not describe that era at all.

These problems have been solved by physically founded dimensional phase transitions [10-12,15,16,48-51]. Thereby, the phase transitions have been modeled locally by four mutually independent physical models. Moreover, the global geometric properties have been described with models using balls or vertices (nodes) and edges [10-12,15,16,52]. Here, we derived general and global geometric and spectral properties of these phase transitions in a geometric manner. That geometric derivation presented here provides additional evidence and additional clarity: In particular, we derived the following physically founded geometric principles:

(1) There is a smallest length L_P that can be observed by a single measurement.

(2) A dimensional phase transition changes the dimension of space.

(3) A dimensional phase transition does not cause a change of volume.

(4) If the largest line segments in a volume have the length $2L_P$, then the dimension of that volume cannot be increased. Thus, the dimensional horizon D_{hori} is reached. At the dimensional horizon D_{hori}, all quantities are at the Planck scale, in particular, each energy is a zero-point energy ZPE equal to one half of the Planck energy E_P.

(5) At D-dimensional space, a ZPO of vacuum has one direction of propagation, $D - 1$ transverse and mutually orthogonal directions of elongation and the volume $V = V_D \cdot \left(Z_{D_{hori} \to D} \cdot L_P \right)^D$.

(6) At a dimensional phase transition from a dimension $D + s$ to a dimension D, there occurs a redshift of the ZPO of the vacuum by the factor $Z_{D_{hori} \to D}$, and transverse elongations in the lost dimensions are lost. Note that objects within space do not experience a redshift at a dimensional phase transition, as they are in space. Whereas the objects of space, the ZPOs of vacuum, instantiate the dimensional distance enlargement factor, whereby they experience the corresponding redshift. Note also, that the increase of the number of the ZPOs of vacuum does not change any single ZPO of vacuum. But the

increase of the number of ZPOs instantiates the expansion of space, so that light and other objects that propagate in space do experience a corresponding redshift.

Moreover, the spectra are founded generally, so they can be applied to the physics at the early universe, to elementary particle physics, to the physics of dark energy, to the derivation of the density of the vacuum or to any other physical system [12,36,37,46].

We used the derived spectrum of the vacuum, in order to derive the density of vacuum (see also [53,54]). Additionally, the density of vacuum as a function of the redshift has been derived from that spectrum. Both results are within the errors of measurement, whereby no fit has been executed. These results provide a clear evidence for the geometrically derived results.

ACKNOWLEDGEMENTS

REFERENCES

[1]. C. Wirtz, Aus der Statistik der Spiralnebel, *Astronomische Nachrichten, 222*, 1924, 33-48.
[2]. E. Hubble, A relation between distance and radial velocity among extra-galactic nebulae, *Proc. of National Acad. of Sciences, 15*, 1929, 168-173.
[3]. A. Einstein, Zur Elektrodynamik bewegter Körper, *Annalen der Physik, 17*, 1905, 891-921.
[4]. A. Einstein, Die Feldgleichungen der Gravitation, *Sitzungsberichte der Königlich Preußischen Akademie der Wissenschaften*, 1915, 844-847.
[5]. A. Einstein, Kosmologische Betrachtungen zur allgemeinen Relativitätstheorie, *Sitzungsberichte der Königlich Preußischen Akademie der Wissenschaften*, 1917, 142-152.
[6]. A. Friedmann, Über die Krümmung des Raumes, *Z. f. Physik, 10*, 1922, 377-386.
[7]. G. Lemaitre, Un Univers homogene de masse constante et de rayon croissant rendant compte de la vitesse radiale des nebuleuses extra-galactiques, Annales de la Societe Scientifique de Bruxelles, A47, 1927, 49-59.
[8]. G. Efstathiou et al. (Planck Collaboration), Planck 2018 results VI. Cosmological parameters, *Astronomy and Astrophysics, 641(A6)*, 2020, 1-67.
[9]. M. Tanabashi et al. (Particle Data Group), Review of particle physics, *Physical Review D, 98(3)*, 2018, 1-1898.
[10]. H.-O. Carmesin, *Vom Big Bang bis heute mit Gravitation – Model for the Dynamics of Space* (Berlin: Verlag Dr. Köster, 2017).
[11]. H.-O. Carmesin, *The Universe Developing from Zero-Point Energy – Discovered by Making Photos, Experiments and Calculations* (Berlin: Verlag Dr. Köster, 2020).
[12]. H.-O. Carmesin, *Cosmological and Elementary Particles Explained by Quantum Gravity* (Berlin: Verlag Dr. Köster, 2021).
[13]. A. H. Guth, Inflationary universe: A possible solution to the horizon and flatness problems, *Physical Review D, 23*, 1981, 347-356.
[14]. M. Zyla et al. (Particle Data Group), Review of particle physics, *Progr. Theor. Exp. Phys., 083C01*, 2020, 1-2092.
[15]. H.-O. Carmesin, *Die Grundschwingungen des Universums – The Cosmic Unification* (Berlin: Verlag Dr. Köster, 2019).
[16]. H.-O. Carmesin, *Quanta of Spacetime Explain Observations, Dark Energy, Gravitation and Nonlocality* (Berlin: Verlag Dr. Köster, 2021).
[17]. H.-O. Carmesin, P. Schöneberg, Droplet Model Used to Analyse the Early Universe, *International Journal of Engineering and Science Invention (IJESI), 11(2)I*, 2022, 58-66.
[18]. M. Lohse et al., Exploring 4D Quantum Hall Physics with a 2D Topological Charge Pump*, Nature, 553*, 2018, 55-58.
[19]. O. Zilberberg et al., Photonic topological pumping the through the edges of a dynamical four-dimensional quantum Hall system*, Nature,553*, 2018, 59-63.
[20]. H.-O. Carmesin, *Entstehung dunkler Energie durch Quantengravitation – Universal Model for Dynamics of Space, Dark Matter and Dark Energy* (Berlin: Verlag Dr. Köster, 2018).
[21]. H.-O. Carmesin, *Entstehung der Raumzeit durch Quantengravitation – Theory for the Emergence of Space, Dark Matter, Dark Energy and Space-Time* (Berlin: Verlag Dr. Köster, 2018).
[22]. S. Perlmutter et al., Discovery of a Supernova Explosion at Half the Age of the Universe*, Nature,391*, 1998, 51-54.
[23]. A. G. Riess, et al., Tests of the Accelerating Universe with Near-Infrared Observations of a High-Redshift Type Ia Supernova, *The Astrophysical Journal, 536*, 2000, 62-67.
[24]. D. W. Pesce et al., The megamaser cosmology project: XIII. Combined Hubble constant constraints, *Astrophysical Journal Letters, 891*, 2020, L1.
[25]. A. G. Riess, et al., Cosmic Distances Calibrated at 1 % Precision with Gaia EDR3 Parallaxes and Hubble Space Telescope Photometry of 75 Milky Way Cepheids Confirm Tension with ΛCDM, *The Astrophysical Journal Letters, 908(L6)*, 2021, 1-11.
[26]. O. Philcox, M. Ivanov, M. Simonovic and M. Zaldarriaga, Combining Full-Shape and BAO Analyses of Galaxy Power Spectra: A 1.6 % CMB-Independent Constraint on H_0, *Journal of Cosmology and Astroparticle Physics, 2020(5)*, 2020, 1-32.
[27]. G. E. Addison, D. J. Watts, C. L. Bennett, M. Halperin, G. Hinshaw, J. L. Weiland, Elucidating ΛCDM: Impact of Baryon Acoustic Oscillation Measurements on the Hubble Constant Discrepancy, *ApJ, 853(2)*, 2018, 1-12.
[28]. T. M. C. Abbott, et al., Dark Energy Survey Year 1 Results: Cosmological Constraints from Galaxy Clustering and Weak Lensing, *Phys. Rev. D, 102*, 2020, 1-34.
[29]. S. Birrer, et al. TDCOSMO: IV. Hierarchical time-delay cosmography - joint inference of the Hubble constant and galaxy density profiles. *Astronomy and Astrophysics, 643*, 2020, 1-40.
[30]. C. Escamilla-Rivera and A. Najera, Dynamical dark energy models in the light of gravitational-wave transient catalogues, *Journal of Cosmology and Astroparticle Physics, 2022(3)*, 2022, 1-60.
[31]. J. P. Blakeslee et al., The Hubble Constant from Infrared Surface Brightness Fluctuation Distances, *The Astrophysical Journal, 911(65)*, 2021, 1-12.
[32]. N. Suzuki, et al., The Hubble Space Telescope Cluster Supernova Survey: V. Improving the Dark Energy Constraints above z > 1 and Building an Early-Type-Hosted Supernova Sample, *ApJ, 746*, 2011, 85-105.
[33]. A. G. Riess et al., A 2.4 % Determination of the Local Value of the Hubble Constant, *The Astrophysical Journal, 826(1)*, 2016, 1-65.

[34]. E. Di Valentino, et al., In the realm of the Hubble tension - a review of solutions, *Class. Quantum Grav., 38*, 2021, 1-110.
[35]. T. Josset, A. Perez, D. Sudarsky, Dark energy as the weight of violating energy conservation, *PRL, 118*, 2017, 233-234.
[36]. H.-O. Carmesin, *Quantum Physics Explained by Gravity and Relativity* (Berlin: Verlag Dr. Köster, 2022).
[37]. H.-O. Carmesin, *The Electroweak Interaction Explained by and Derived from Gravity and Relativity* (Berlin: Verlag Dr. Köster, 2022).
[38]. A. G. Riess, et al., A Comprehensive Measurement of the Local Value of the Hubble Constant with 1 km s^{-1} Mpc^{-1} Uncertainty from the Hubble Space Telescope and the SHOES Team, *arXiv, 2112.04510v2*, 2022, 1-67.
[39]. H.-O. Carmesin, *Modeling of SN1a data with my theory* (URL: https://www.researchgate.net/publication/351093848_H0_20 210424pdf#fullTextFileContent, 2021).
[40]. R. B. Tully, H. Courtois, Y. Hoffmann and D. Pomerede, The Laniakea supercluster of galaxies, *Nature, 513(7516)*, 2014, 71-74.
[41]. A. Dupuy et al., Partitioning the Universe into gravitational basins using the cosmic velocity field, *MNRAS, 489*, 2019, L1-L6.
[42]. G. Chon and H. Böhringer and S. Zaroubi, On the definition of superclusters, *Astronomy and Astrophysics, L14*, 2015, 1-5.
[43]. H. Böhringer, G. Chon, M. Bristow and C. A. Collins, The extended ROSAT-ESO Flux-Limited X-Ray Galaxy Cluster Survey (REFLEX II), *Astronomy and Astrophysics, 574(A26)*, 2015, 1-8.
[44]. E. L. Turner, R. Cen and J. P. Ostriker, The relation of local measures of Hubble's constant to its global value, *The Astronomical Journal, 103(5)*, 1992, 1427-1437.
[45]. H.-O. Carmesin, Physical Explanation of the H_0 – Tension, *International Journal of Engineering and Science Invention (IJESI), 10(8) II*, 2021, 34-38.
[46]. H.-O. Carmesin, *The Elementary Charge Explained by Quantum Gravity* (Berlin: Verlag Dr. Köster, 2021).
[47]. H.-O. Carmesin, The Origin of the Energy. *PhyDid B*, 2021, 29-34.
[48]. H.-O. Carmesin, A Model for the Dynamics of Space - Expedition to the Early Universe, *PhyDid B, FU Berlin, hal-02077596*, 2018, 1-9.
[49]. H.-O. Carmesin, Explanation of the Rapid Enlargement of Distances in the Early Universe. *PhyDid B*, 2020, 11-17.
[50]. L. Heeren, P. Sawitzki, H.-O. Carmesin, Comprehensive Derivation of a Density Limit in the Evolution of Space, *PhyDid B*, 2020, 39-42.
[51]. P. Sawitzki, H.-O. Carmesin, Dimensional transitions in a Bose gas, *PhyDid B, FU Berlin*, 2021, 53-59.
[52]. P. Schöneberg, H.-O. Carmesin, Solution of a Density Problem in the Early Universe. *PhyDid B*, 2020, 43-46.
[53]. H.-O. Carmesin, A Novel Equivalence Principle for Quantum Gravity. *PhyDid B*, 2019, 1-9.
[54]. H.-O. Carmesin, Lernende erkunden die Raumzeit. *Der Mathematikunterricht, 2*, 2021, 47-56.